

Diquark-diquark correlations in the 1S_0 $\Lambda\Lambda$ potential

T. Fernández-Caramés⁽¹⁾, A. Valcarce⁽²⁾, and P. González⁽¹⁾

(1) *Dpto. de Física Teórica and IFIC*

Universidad de Valencia - CSIC, E-46100 Burjassot, Valencia, Spain

(2) *Grupo de Física Nuclear and IUFFyM*

Universidad de Salamanca, E-37008 Salamanca, Spain

Abstract

We derive a $\Lambda\Lambda$ potential from a chiral constituent quark model that has been successful in describing one, two and three nonstrange baryon systems. The resulting interaction at low energy is attractive at all distances due to the σ exchange term. The attraction allows for a slightly bound state just below the $\Lambda\Lambda$ threshold. No short-range repulsive core is found. We extract the diquark-diquark contribution that turns out to be the most attractive and probable at small distances. At large distances the asymptotic behavior of the $\Lambda\Lambda$ interaction provides a prediction for the $\sigma\Lambda\Lambda$ coupling constant.

Keywords: diquarks, chiral constituent quark models, $\Lambda\Lambda$ interaction

Pacs: 12.39.Jh, 12.39.Pn, 14.20.Pt

The $\Lambda\Lambda$ interaction has been the object of extensive consideration. On the one hand the knowledge of the $\Lambda\Lambda$ altogether with the $N\Lambda$ interaction is a necessary ingredient to obtain a physical description of hypernuclei for which binding energies have been measured [1]. On the other hand the $\Lambda\Lambda$ 1S_0 channel has the quantum numbers of the H -dibaryon, theoretically predicted almost thirty years ago with a mass below the $\Lambda\Lambda$ threshold [2] and not experimentally identified until now [3].

Since Λ targets are not available there is not direct measurement of the $\Lambda\Lambda$ scattering process. Indirect information can be extracted from the scarce old Λp scattering data [4] and from measured binding energies of $\Lambda\Lambda$ hypernuclei [1]. Approaches to the $\Lambda\Lambda$ interaction potential have been pursued at the baryon and quark levels. At the baryon level phenomenological (in the sense of reproducing some indirect experimental information) meson-exchange (σ and ω) potentials have been constructed [5–7]. At the quark level, gluon dominant (only one-gluon exchange between quarks), pure chiral (only meson exchanges between quarks) and chiral constituent quark (gluon plus meson exchanges) models have been used [8]. Finally, hybrid models where some pieces of the interaction (usually the gluon and pion exchanges) are considered at the quark level while others (usually the one-sigma exchange) are parametrized at the baryonic level [9], with several free parameters fitted differently for different observables (deuteron binding energy, NN singlet S -wave phase shifts, NN P -wave phase shifts and hyperon-nucleon interaction), have been also efficient to describe data.

A quite general conclusion arising from the quark approaches until now is that the interaction between two Λ 's presents a repulsive core [8]. Though this conclusion is easily understood in a gluon dominant model by comparison to the NN case (the interaction generated at short distances by the one-gluon exchange is repulsive) it seems more controversial in chiral constituent quark models incorporating the σ -meson exchange, responsible for the correct medium range behavior in the NN system and attractive at all distances, where it may be dominant.

Comparatively phenomenological baryonic interactions can be very precise when a sufficient amount of data are at disposal (the interaction parameters depending on the specific case under consideration), however quark treatments can be fully predictive since the same potential parameters (fixed once for all, for instance, in the well-known nonstrange sector) could be applied to any other baryon-baryon system. To this respect we should first realize that at the quark level only a chiral constituent quark model can provide a realistic description of nonstrange two-baryon systems. The gluon dominant model is not able to reproduce the long-distance behavior of the NN interaction. The pure chiral models lack, when applied to the NN interaction, of the necessary medium range attraction [10]. Then we are left with chiral constituent quark models where the appearance or not of a repulsive core in the $\Lambda\Lambda$ interaction will depend on the interplay between gluon and meson exchanges, i.e., on the relative intensity of the one gluon and the meson exchange terms in the potential. This relative intensity can be fixed, once a chiral realization of QCD at low energy is chosen, by the requirement of having the most accurate description of one and two-body systems.

In this letter we revise the conclusions obtained about the $\Lambda\Lambda$ system by means of a chiral constituent quark model tightly constrained by the description of the nonstrange sector and the strange meson and baryon spectra.

In the last years a high degree of precision has been reached in the description of the

nonstrange one, two and three baryon systems by means of a $SU(2) \times SU(2)$ chiral constituent quark model (as originally named in reference [11]) containing π and σ exchanges plus a residual one-gluon exchange interaction [12]. We shall call this model hereforth CCM [11]. This strong interaction model corresponds to a nonrelativistic approach to an effective theory incorporating quarks, gluons and Goldstone bosons [13], the effectiveness of the CCM parameters hopefully giving account, in an effective manner, of effects out of the scope of our approach. A main difference with other models with a *similar* content [14] is the consistent treatment, at the level of the wave function, of the baryon-baryon interaction and the baryon spectra. Another basic difference comes from the requirement to describe a wide number of observables, restricting very much the possible values of the parameters. The predictive power of the CCM has been tested in its successful application to the NN , $N\Delta$, tritium and nonstrange baryon spectra. The model has a reduced relative intensity of the gluon against meson exchanges, as compared to the other models. Gluon and pion contribute both about half of the $\Delta - N$ mass difference and the short-range NN repulsion in the S -wave comes mainly from the pion term at difference with other models where the gluon, through configuration mixing, provides the major contribution. This shows that *similar* models, in the sense of using a similar form of the interaction, may give rise to very different physical descriptions.

In order to apply the CCM to the $\Lambda\Lambda$ case an extension to deal with strange baryons is required. Besides confinement and gluon terms the minimal chiral extension used in the literature comprises the exchange of a singlet scalar meson, the σ (mediating light-strange and strange-strange as well as light-light quark interactions) and a pseudoscalar octet involving pions, kaons and eta. The motivation for this systematic is the following. From existing baryonic analysis the σ and ω exchanges seem to be the most relevant ones. At the quark level one expects that quark antisymmetrization effects play a similar role to the baryonic ω exchange. Indeed at the baryon level the ω provides the short-range repulsion in the NN interaction whilst at the quark level antisymmetrization effects on the gluon and π terms provide to a great extent the same effect. The consideration of an $SU(3) \times SU(3)$ chiral model would incorporate an octet of scalar mesons as well. However the scalar masses, with the exception of the singlet σ ($f_0(600)$), are significantly higher than the pseudoscalar octet ones what makes plausible their contributions to be less important. This way of proceeding results in an extended model that fits well the strange hadron spectra [15] while keeping the successful description for the nonstrange systems.

Explicitly the quark-quark interaction reads:

$$V_{qq}(\vec{r}_{ij}) = V_{CON}(\vec{r}_{ij}) + V_{OGE}(\vec{r}_{ij}) + V_{\pi}(\vec{r}_{ij}) + V_{\sigma}(\vec{r}_{ij}) + V_K(\vec{r}_{ij}) + V_{\eta}(\vec{r}_{ij}) , \quad (1)$$

where the i and j indices are associated with i and j quarks, respectively, and \vec{r}_{ij} stands for the interquark distance.

The confinement potential is chosen linear,

$$V_{CON}(\vec{r}_{ij}) = -a_c \vec{\lambda}_i \cdot \vec{\lambda}_j r_{ij} , \quad (2)$$

where a_c is the confinement strength, the $\vec{\lambda}$'s are the $SU(3)$ color matrices, and the color structure prevents from having confining interaction between color singlets.

From the nonrelativistic reduction of the one-gluon-exchange diagram in QCD for point-like quarks one gets,

$$V_{OGE}(\vec{r}_{ij}) = \frac{1}{4} \alpha_s \vec{\lambda}_i \cdot \vec{\lambda}_j \left\{ \frac{1}{r_{ij}} - \frac{1}{4} \left(\frac{1}{2m_i^2} + \frac{1}{2m_j^2} + \frac{2}{3m_i m_j} \vec{\sigma}_i \cdot \vec{\sigma}_j \right) \frac{e^{-r/r_0}}{r_0^2 r_{ij}} \right\}, \quad (3)$$

where α_s is an effective strong coupling constant and m_i is the mass of the quark i . $\vec{\sigma}_i$ stands for the Pauli spin operator. Let us realize that the contact term involving a Dirac $\delta(\vec{r})$ that comes out in the deduction of the potential has been regularized in the form

$$\delta(\vec{r}) \rightarrow \frac{1}{4\pi r_0^2} \frac{e^{-r/r_0}}{r}, \quad (4)$$

giving rise to the second term of Eq. (3) (r_0 is a regularization parameter). This avoids to get an unbound baryon spectrum from below when solving the Schrödinger equation [16].

The static pion and sigma exchange potentials are given by:

$$V_\pi(\vec{r}_{ij}) = \frac{1}{3} \frac{g_{ch}^2}{4\pi} \frac{m_\pi^2}{4m_i m_j} \frac{\Lambda_\chi^2}{\Lambda_\chi^2 - m_\pi^2} m_\pi \left[Y(m_\pi r_{ij}) - \frac{\Lambda_\chi^3}{m_\pi^3} Y(\Lambda_\chi r_{ij}) \right] \vec{\sigma}_i \cdot \vec{\sigma}_j \vec{\tau}_i \cdot \vec{\tau}_j, \quad (5)$$

$$V_\sigma(\vec{r}_{ij}) = -\frac{g_{ch}^2}{4\pi} \frac{\Lambda_\chi^2}{\Lambda_\chi^2 - m_\sigma^2} m_\sigma \left[Y(m_\sigma r_{ij}) - \frac{\Lambda_\chi}{m_\sigma} Y(\Lambda_\chi r_{ij}) \right], \quad (6)$$

where g_{ch} is the chiral coupling constant, Λ_χ is a cut-off parameter and the $\vec{\tau}$'s are the isospin quark Pauli matrices. m_π and m_σ are the masses of the pseudoscalar and scalar Goldstone bosons, respectively. $Y(x)$ is the standard Yukawa function defined by $Y(x) = e^{-x}/x$. The *new* kaon and eta potentials read

$$V_K(\vec{r}_{ij}) = \frac{1}{3} \frac{g_{ch}^2}{4\pi} \frac{m_K^2}{4m_i m_j} \frac{\Lambda_K^2}{\Lambda_K^2 - m_K^2} m_K \left[Y(m_K r_{ij}) - \frac{\Lambda_K^3}{m_K^3} Y(\Lambda_K r_{ij}) \right] (\vec{\sigma}_i \cdot \vec{\sigma}_j) \sum_{a=4}^7 (\lambda_i^a \cdot \lambda_j^a),$$

$$V_\eta(\vec{r}_{ij}) = \frac{1}{3} \frac{g_{ch}^2}{4\pi} \frac{m_\eta^2}{4m_i m_j} \frac{\Lambda_\eta^2}{\Lambda_\eta^2 - m_\eta^2} m_\eta \left[Y(m_\eta r_{ij}) - \frac{\Lambda_\eta^3}{m_\eta^3} Y(\Lambda_\eta r_{ij}) \right] (\vec{\sigma}_i \cdot \vec{\sigma}_j) [\cos\theta_p (\lambda_i^8 \cdot \lambda_j^8) - \sin\theta_p],$$

where the angle θ_p appears as a consequence of considering the physical η instead the octet one.

Let us keep in mind that the values of the parameters for confinement, gluon, pion and sigma exchanges are fixed from the nonstrange sector [12]. For kaon and eta exchanges the parameters are fixed from a fit to the strange meson spectra [15]. In Table I we compile the values used. Let us note that our cutoff parameter for the kaon and the eta is different than for sigma and pion. This comes from a fine tune to the strange meson spectra but it will not be quantitatively relevant for the $\Lambda\Lambda$ interaction.

The general nonrelativistic framework to obtain the $\Lambda\Lambda$ potential from the quark-quark interaction is the Resonating Group Method (RGM). A much more simplified treatment, the adiabatic or Born-Oppenheimer (BO) approximation, can be suitable under the assumption that the quarks move inside the baryonic clusters much faster than the clusters relative to

each other. Since applications of RGM and BO to the nonstrange systems do not show any relevant difference [17] we shall adhere hereforth to a BO approach. The resulting potential can be obtained as:

$$V_{B_1 B_2(LST) \rightarrow B_3 B_4(L'S'T)}(R) = \mathcal{V}_{LST}^{L'S'T}(R) - \mathcal{V}_{LST}^{L'S'T}(\infty), \quad (7)$$

where

$$\mathcal{V}_{LST}^{L'S'T}(R) = \frac{\langle \Psi_{B_1 B_2}^{L'S'T}(\vec{R}) | \sum_{i < j=1}^6 V_{qq}(\vec{r}_{ij}) | \Psi_{B_3 B_4}^{LST}(\vec{R}) \rangle}{\sqrt{\langle \Psi_{B_1 B_2}^{L'S'T}(\vec{R}) | \Psi_{B_1 B_2}^{L'S'T}(\vec{R}) \rangle} \sqrt{\langle \Psi_{B_3 B_4}^{LST}(\vec{R}) | \Psi_{B_3 B_4}^{LST}(\vec{R}) \rangle}}, \quad (8)$$

with $\Psi_{B_i B_j}^{LST}(\vec{R})$ given in general (B_i and B_j can be nonidentical baryons) by

$$\begin{aligned} \Psi_{B_1 B_2}^{LST}(\vec{R}) = & \frac{\mathcal{A}}{\sqrt{1 + \delta_{B_1 B_2}}} \sqrt{\frac{1}{2}} \left\{ \left[\Phi_{B_1} \left(123; -\frac{\vec{R}}{2} \right) \Phi_{B_2} \left(456; \frac{\vec{R}}{2} \right) \right]_{LST} \right. \\ & \left. + (-1)^f \left[\Phi_{B_2} \left(123; -\frac{\vec{R}}{2} \right) \Phi_{B_1} \left(456; \frac{\vec{R}}{2} \right) \right]_{LST} \right\}, \quad (9) \end{aligned}$$

where f (even or odd) determines the baryon-baryon symmetry and S , T and L correspond to the total spin, isospin and orbital angular momentum of the two-baryon system. \mathcal{A} is the six-quark antisymmetrizer written as [18]

$$\mathcal{A} = \left(1 - \sum_{i=1}^2 \sum_{j=4}^5 P_{ij} - P_{36} \right) (1 - \mathcal{P}), \quad (10)$$

where we have identified quarks 3 and 6 as the strange ones in each baryon. P_{ij} is the operator that exchanges particles i and j and \mathcal{P} exchanges the two clusters. P_{ij} can be explicitly written as the product of permutation operators in color (C), spin-isospin (ST) and orbital (O) spaces,

$$P_{ij} = P_{ij}^C P_{ij}^{ST} P_{ij}^O. \quad (11)$$

The subtraction of $\mathcal{V}_{LST}^{L'S'T}(\infty)$ assures that no internal cluster energies enter in the baryon-baryon interacting potential.

The total wave function of a single baryon cannot be in the $\Lambda\Lambda$ case, at difference with the NN one, separated in orbital, spin and color parts. Whereas one can isolate the color part one has to maintain the orbital and flavor structure altogether due to the flavor (mass) dependence of the orbital part. Hence the Λ wave function reads

$$\Phi_{\Lambda}(\vec{r}_1, \vec{r}_2, \vec{r}_3; \vec{R}/2) = \frac{1}{\sqrt{2}} \left(\phi^{MS} \chi^{MS} + \phi^{MA} \chi^{MA} \right) \otimes \xi, \quad (12)$$

ϕ , χ , and ξ standing for the orbital-flavor, spin and color parts, respectively. The orbital wave function for a quark i in a cluster at position $\vec{R}/2$ is chosen as

$$\varphi(\vec{r}_i, \vec{R}/2) = \left(\frac{1}{\pi b_i^2} \right)^{3/4} \exp \left(-\frac{(\vec{r}_i - \vec{R}/2)^2}{2b_i^2} \right). \quad (13)$$

The dependence on the quark mass enters in the parameter b_i . We shall assume $1/(m_s b_s^2) = 1/(m_{u,d} b_{u,d}^2)$ in order to have the same kinetic energy for all quarks in the baryon.

The result for the 1S_0 potential is drawn in Fig. 1 where the contributions from σ , π , η and gluon exchanges are also depicted. Note that the kaon contribution vanishes due to isospin conservation in the possible quark-kaon-quark vertices. As can be seen the dominant contribution is attractive and comes from the σ . Actually it corresponds to a pure σ baryonic potential since no quark-exchanges (related to the P_{kl} terms in the antisymmetrizer) contribute either to the numerator or denominator in (8). Let us realize that except for the small differences coming from the exchange contribution in the NN case and the strange quark mass in the $\Lambda\Lambda$ one, this interaction should be, as in fact it is, quantitatively very similar in the NN and $\Lambda\Lambda$ cases.

The gluon contribution comes only from quark exchanges, since being the gluon a color octet cannot directly connect two baryons (color singlet states). Furthermore the only surviving gluonic contribution comes from the chromomagnetic part being repulsive. The strength of this repulsion is smaller (about one third for $R = 0.01$ fm) than the corresponding one in NN . This is due, on the one hand, to the lesser number of diagrams contributing (no exchanges involving light-strange quarks are possible) and, on the other hand, to the strange quark mass factors in the OGE potential. Despite this we can immediately understand why the $\Lambda\Lambda$ interaction has a repulsive core in other chiral constituent quark models where the gluon term is dominant. As a matter of fact if we multiply our gluon coupling constant by a factor 2 and rearrange correspondingly the chiral coupling constant, a repulsive core would be obtained (at the prize of destroying the good description of many other observables).

Regarding the π term it is repulsive as in NN . However as for $\Lambda\Lambda$ it only contributes, due to its isovector character, through quark exchanges, the repulsion is much weaker (about one fifth for $R = 0.01$ fm). Indeed, in the $\Lambda\Lambda$ case the pion contribution turns out to be less important than the gluon one and much less important in absolute value than the σ one. Hence the attraction provided by the σ -exchange surpasses the gluon+pion repulsion. This net attraction cannot be compensated by the small repulsive contribution from the η -exchange. To this respect it is also interesting to look at the results for $N\Lambda \rightarrow N\Lambda$ (see below).

Since the values of the parameters m_s and $\Lambda_{\eta,K}$ are fitted only from spectroscopy it is convenient to test the sensitivity of our results to changes in them. As mentioned before the effect of taking $\Lambda_{\eta,K}$ different from Λ_χ is small, about 5% in the values of the potential at most. Regarding m_s a variation of 150 MeV around the chosen value gives rise to a modification of the potential of a 15% at most. This gives us confidence in the results we obtain whose qualitative character is essentially determined by the well fitted $SU(2) \times SU(2)$ parameters.

Once we have determined the $\Lambda\Lambda$ interacting potential we proceed to the study of bound states. For this purpose the method of the Fredholm determinant is particularly simple and trustable: starting from the Lippmann-Schwinger equation for the $\Lambda\Lambda$ system,

$$\int d^3k'' \left[\delta(\vec{k}' - \vec{k}'') - \frac{\langle \vec{k}' | V | \vec{k}'' \rangle}{E - E_{k''}} \right] \langle \vec{k}'' | T(E) | \vec{k} \rangle = \langle \vec{k}' | V | \vec{k} \rangle, \quad (14)$$

where $|\vec{k}\rangle$ stands for a momentum state of $\Lambda\Lambda$, and substituting the integral by a N -point quadrature we can formally write:

$$[T(E)] = \frac{[V]}{[1 - VG_0(E)]}, \quad (15)$$

where $G_0(E) = 1/(E - \vec{p}^2/2\mu)$ (μ is the reduced mass of the system) is the nonrelativistic propagator. Then a bound state, corresponding to a pole of the T -matrix in the real axis, leads to

$$\det [1 - VG_0(E)] = 0, \quad (16)$$

whose solution determines the binding energy [19].

In Fig. 2 the value of the Fredholm determinant as a function of energy is depicted. As we can see there appears only one possible bound state very close to the $\Lambda\Lambda$ threshold (with a binding energy of 0.022 MeV). This is in agreement with upper bounds extracted from $\Lambda\Lambda$ hypernuclei [1] but in contradiction with previous quark model results obtaining much more binding what was associated to the presence of a tightly bound H -dibaryon [8]. Although to analyze the H -dibaryon a coupled channel calculation should be performed, when this is done, the probabilities of the $\Lambda\Lambda$, $N\Xi$ and $\Sigma\Sigma$ components do not differ much from the initial flavor $SU(3)$ Clebsch-Gordan coefficients [8,9]. This comes from the fact that the coupling between the $\Lambda\Lambda$, $N\Xi$ and $\Sigma\Sigma$ is very small, all the direct diagrams do not contribute (except for the pion between $\Lambda\Lambda$ and $\Sigma\Sigma$, but giving a small contribution due to the different symmetry of the spin wave function), the coupling mainly generated by the exchange diagrams that are very short-ranged as to give an important contribution to the binding. Therefore the binding is mainly driven by the sigma-meson exchange in each two-body channel separately. Therefore we might infer, from our one-channel calculation, that a tightly bound H -dibaryon as obtained with *similar* quark models may not be justified. According to our result the experimental absence of such state could be related to the well known difficulty to disentangle in partial wave analysis the existence of a resonance close to a threshold (this is nowadays very much discussed regarding the nature of some mesons as could be, for example, the $X(3872)$, that it is precisely in the D^0D^{*0} threshold).

On the theoretical side there has been also suggested that inner diquark structures could prevent, through Pauli repulsion at very short distances, such a tight binding [20]. Then it may be instructive to perform an analysis of the diquark contributions to our $\Lambda\Lambda$ interaction. We can easily isolate components containing diquark-diquark structures from the $\Lambda\Lambda$ wave function written above. In fact any Λ wave function contains a diquark, say a pair of quarks in a $[1]_{\text{spin}} - [\bar{3}]_{\text{flavor}} - [\bar{3}]_{\text{color}}$ configuration, through the term $\phi^{MA}\chi^{MA}$ in equation (12). The contribution of these components to the $\Lambda\Lambda$ potential is shown in Fig. 3. As can be checked it is attractive at all distances and strongly attractive at short distances mainly due to the gluonic Coulomb term and to a less extent to the σ exchange. This short-range attractive contribution (reduced by some repulsion from the rest of the components) determines the

short-range attractive character of the $\Lambda\Lambda$ potential. Actually the component containing diquark-diquark becomes the dominant one when reducing the interbaryon distance. This can be seen by defining a diquark-diquark probability depending on the interbaryon distance R as the ratio

$$P(R) = \frac{\langle (\phi^{MA}\chi^{MA})_{\Lambda} (\phi^{MA}\chi^{MA})_{\Lambda} | \mathcal{A} | (\phi^{MA}\chi^{MA})_{\Lambda} (\phi^{MA}\chi^{MA})_{\Lambda} \rangle}{4 \langle \Phi_{\Lambda}\Phi_{\Lambda} | \mathcal{A} | \Phi_{\Lambda}\Phi_{\Lambda} \rangle}, \quad (17)$$

where we have used $\mathcal{A}^2 = \mathcal{A}$. This probability appears in Fig. 4 where it is clear its increasing from the nonoverlapping value 0.25 to almost 0.5 at very short interbaryonic distances as it corresponds to the bosonic diquark character (as a counterpart the other non-diquark-diquark components show an opposite tendency). Therefore we do not see in our analysis any signature of a strong Pauli diquark blocking at short distances. This stems from the diquark-diquark structure we are dealing with. Since both symmetric and antisymmetric color states are allowed no restriction on the two identical diquark orbital angular momentum comes out (quite a different situation one has in the hypothetical pentaquark case where only the antisymmetric color state is allowed). Therefore we conclude that the bound state found does not owe its loose binding to Pauli diquark repulsion at very short distances but instead to the diquark-diquark dynamics. If combined with the assumption that the three-diquark component is dominant for the H -dibaryon such dynamics could explain its non-appearance as a tightly bound state.

Finally, our results allow also for a direct determination of the $\sigma\Lambda\Lambda$ coupling constant from the σqq one since at long distances, where there is not any significant baryon overlap, the σ -exchange potential can be identified with a σ -exchange at the baryon level that can be parametrized as,

$$V_{\sigma}^{\Lambda\Lambda\rightarrow\Lambda\Lambda}(R) = -\frac{g_{\sigma\Lambda\Lambda}^2}{4\pi} \frac{\Lambda_{\chi}^2}{\Lambda_{\chi}^2 - m_{\sigma}^2} \frac{e^{-m_{\sigma}R}}{R}. \quad (18)$$

In order to eliminate as much as possible the model dependence and to do a non-meaningless comparison of our results with others in the literature it is convenient to take the ratio to the NN case [21]. Thus we get,

$$\frac{g_{\sigma\Lambda\Lambda}}{g_{\sigma NN}} = 0.88. \quad (19)$$

Let us emphasize that this ratio reflects precisely the different wave function structure of N and Λ as a consequence of the $SU(3)$ quark mass breaking. Our ratio is significantly bigger than the one predicted by some baryonic models [22] but in agreement with others [6,9,23,24]. Since all baryonic models give a reasonable description of the scarce $N\Lambda$ data one cannot discriminate between them. This rather points out the need for more precise data. For the sake of completeness we study the $N\Lambda$ potential with our model. The result is shown in Fig. 5. As can be checked the interaction becomes slightly repulsive at short distances due to the dominance of the pion plus mainly gluon repulsion against the sigma attraction. Actually the pion and gluon contributions are about twice those in $\Lambda\Lambda$ whereas the σ contributions remain more or less the same. In Fig. 6 we compare our $N\Lambda$ potential with the Nijmegen interactions F and D [25]. As can be seen they are quite similar for

$R \geq 1.3$ fm. In the $\Lambda\Lambda$ case our results are definitely closer to the predictions by Nijmegen interaction D.

In summary, by using a chiral constituent quark model precisely fitted in the nonstrange sector to a bulk of baryon, meson and baryon-baryon data, we have shown that, contrary to what has been usually assumed in baryonic models and calculated in previous quark models, the $\Lambda\Lambda$ interaction in the 1S_0 partial wave is attractive at short distances. In our CCM this attraction comes from the σ exchange, whose effect cannot be surmounted even at short distances by the gluon + pion + eta repulsion. The different short-range behavior as compared to the NN case is understood from the very different quantitative role played by pion + gluon exchanges against sigma exchange in both cases. Actually in the “intermediate” NA case our model interaction becomes repulsive at short distances in agreement with previous treatments and suggestions from data. We predict a slightly bound $\Lambda\Lambda$ state whose energy fits well inside the upper bounds imposed from $\Lambda\Lambda$ hypernuclei data. This is encouraging to try to obtain a microscopic description of $\Lambda\Lambda$ hypernuclei for which we have not at the current moment a satisfactory explanation. To this respect to have at disposal the $\Lambda\Lambda$, NA and NN interactions obtained on the same footing may be extremely valuable.

From the point of view of quark flavor-color configurations the $\Lambda\Lambda$ attraction is mainly related to a structure containing two diquarks. The involved diquark-diquark dynamics giving rise to the loosely bound state could also provide an explanation for the experimental absence of a tightly bound H -dibaryon. We have also derived a $g_{\sigma\Lambda\Lambda}$ coupling being almost 90% of $g_{\sigma NN}$ as a reflection of the assumed $SU(3)$ breaking.

Certainly there are not at present precise data to check the $\Lambda\Lambda$ short-range character and consequently our model against others. Despite this we think it is worth to pursue a theoretical program aiming at the examination of the consequences derived from it and their possible experimental checks. This can be important not only to directly progress in the understanding of the $\Lambda\Lambda$ system but also (due to the connection of the short-range character to the gluon intensity) to indirectly disentangle the quantitative role played by gluons and pions in the NN system.

ACKNOWLEDGMENTS

This work was partially funded by Dirección General de Investigación Científica y Técnica (DGICYT) under the Contract No. BFM2001-3563, by Junta de Castilla y León under the Contract No. SA104/04, and by Oficina de Ciencia y Tecnología de la Comunidad Valenciana, Grupos03/094.

REFERENCES

- [1] H. Takahashi *et al.*, Phys. Rev. Lett. **87**, 212502 (2001); J.K. Ahn *et al.*, Phys. Rev. Lett. **87**, 132504 (2001); M. Danysz *et al.*, Nucl. Phys. **49**, 121 (1963); S. Aoki *et al.*, Prog. Theor. Phys. **85**, 1287 (1991).
- [2] R.L. Jaffe, Phys. Rev. Lett. **38**, 195 (1977).
- [3] R.E. Chrien, Proceedings of International Conference on Quark Lepton Nuclear Physics, QULEN'97, Osaka, Japan (1997); B. Bassalleck, Proceedings of the 6th International Conference on the Intersections of Particle and Nuclear Physics, Big Sky, Montana (1997).
- [4] G. Alexander *et al.*, Phys. Rev. **173**, 1452 (1968); B. Sechi-Zorn *et al.*, Phys. Rev. **175**, 1735 (1968); J.A. Kadyk *et al.*, Nucl. Phys. B **27**, 13 (1971).
- [5] V.G.J. Stoks and T.A. Rijken, Phys. Rev. C **59**, 3009 (1999).
- [6] A. Reuber, K. Holinde, and J. Speth, Nucl. Phys. A **570**, 543 (1994).
- [7] J. Caro, C. García-Recio, and J. Nieves, Nucl. Phys. A **646**, 299 (1999).
- [8] T. Sakai, K. Shimizu, and K. Yazaki, Prog. Theor. Phys. Suppl. **137**, 121 (2000), and references therein.
- [9] U. Straub, Z.Y. Zhang, K. Braüer, A. Faessler, S.B. Khadkikar, and G. Lübeck, Nucl. Phys. A **483**, 686 (1988).
- [10] C. Nakamoto and H. Toki, Prog. Theor. Phys. **99**, 1001 (1998).
- [11] F. Fernández, A. Valcarce, U. Straub, and A. Faessler, J. Phys. G **19**, 2013 (1993); A. Valcarce, P. González, F. Fernández, and V. Vento, Phys. Lett. B **367**, 35 (1995).
- [12] A. Valcarce, H. Garcilazo, F. Fernández, and P. González, Rep. Prog. Phys. **68**, 965 (2005), and references therein.
- [13] A. Manohar and V. Georgi, Nucl. Phys. B **234**, 189 (1984).
- [14] K. Shimizu and M. Koyama, Nucl. Phys. A **646**, 211 (1999).
- [15] J. Vijande, F. Fernández, and A. Valcarce, J. Phys. G **31**, 481 (2005).
- [16] R.K. Bhaduri, L.E. Cohler, and Y. Nogami, Phys. Rev. Lett. **44**, 1369 (1980).
- [17] H. Garcilazo, A. Valcarce, and F. Fernández, Phys. Rev. C **60**, 044002 (1999).
- [18] K. Holinde, Nucl. Phys. A **415**, 477 (1984).
- [19] A. Valcarce, H. Garcilazo, and F. Fernández, Phys. Rev. C **52**, 539 (1995).
- [20] R.L. Jaffe and F. Wilczek, Phys. Rev. Lett. **91**, 232003 (2003).
- [21] B. Juliá-Díaz, A. Valcarce, P. González, and F. Fernández, Phys. Rev. C **66**, 024005 (2002).
- [22] K. Holinde, H.C. Kim, A. Reuber, and J. Speth, Nucl. Phys. A **585**, 149c (1995); A. Reuber, K. Holinde, H.C. Kim, and J. Speth, Nucl. Phys. A **608**, 243 (1996).
- [23] P.M.M. Maessen, T.A. Rijken, and J.J. de Swart, Phys. Rev. C **40**, 2226 (1989); M.M. Nagels, T.A. Rijken, and J.J. de Swart, Phys. Rev. D **12**, 744 (1975), Phys. Rev. D **15**, 2547 (1977), Phys. Rev. D **20**, 1633 (1979).
- [24] B. Holzenkamp, K. Holinde, and J. Speth, Nucl. Phys. A **500**, 485 (1989).
- [25] Y. Yamamoto, T. Motoba, H. Himeno, K. Ikeda, and S. Nagata, Prog. Theor. Phys. Suppl. **117**, 361 (1994), and references therein.

TABLES

TABLE I. Quark-model parameters.

$m_{u,d}$ (MeV)	313	α_s	0.54
m_s (MeV)	555	r_0 (fm ⁻¹)	0.18
m_π (fm ⁻¹)	0.7	a_c (MeV fm ⁻¹)	185.0
m_σ (fm ⁻¹)	3.42	$g_{ch}^2/4\pi$	0.54
m_K (fm ⁻¹)	2.51	Λ_χ (fm ⁻¹)	4.2
m_η (fm ⁻¹)	2.77	$\Lambda_K = \Lambda_\eta$ (fm ⁻¹)	5.2
θ_p (°)	-15		

FIGURES

FIG. 1. 1S_0 $\Lambda\Lambda$ potential. The contribution of the different terms in Eq. (1) has been depicted.

FIG. 2. Fredholm determinat of the $\Lambda\Lambda$ system with $J = 0$ as a function of the nonrelativistic energy E .

FIG. 3. Diquark-diquark contributions to the 1S_0 $\Lambda\Lambda$ potential. We have shown separately the most important terms in Eq. (1).

FIG. 4. Diquark-diquark probability in the 1S_0 $\Lambda\Lambda$ wave function as a function of the inter-baryon distance R . The solid line represents the probability of the diquark-diquark component and the dashed line the probability of any other non-diquark-diquark components.

FIG. 5. 1S_0 $N\Lambda$ potential.

FIG. 6. (a) Comparison of the quark-model based 1S_0 $N\Lambda$ potential to the Nijmegen model (crosses stand for model F and circles for model D) of Ref. [25]. (b) Same as (a) for the 1S_0 $\Lambda\Lambda$ potential.

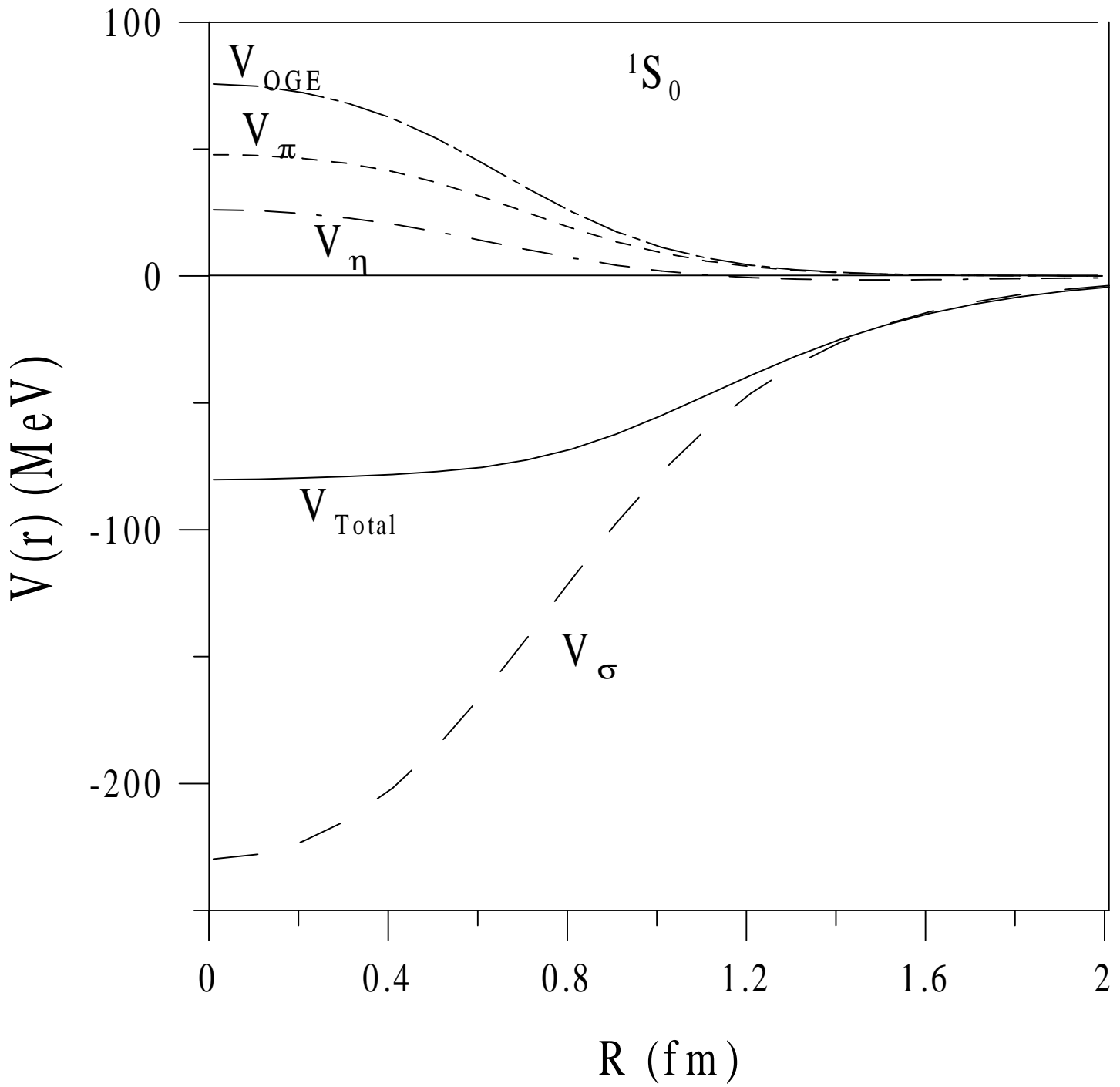


Figure 1

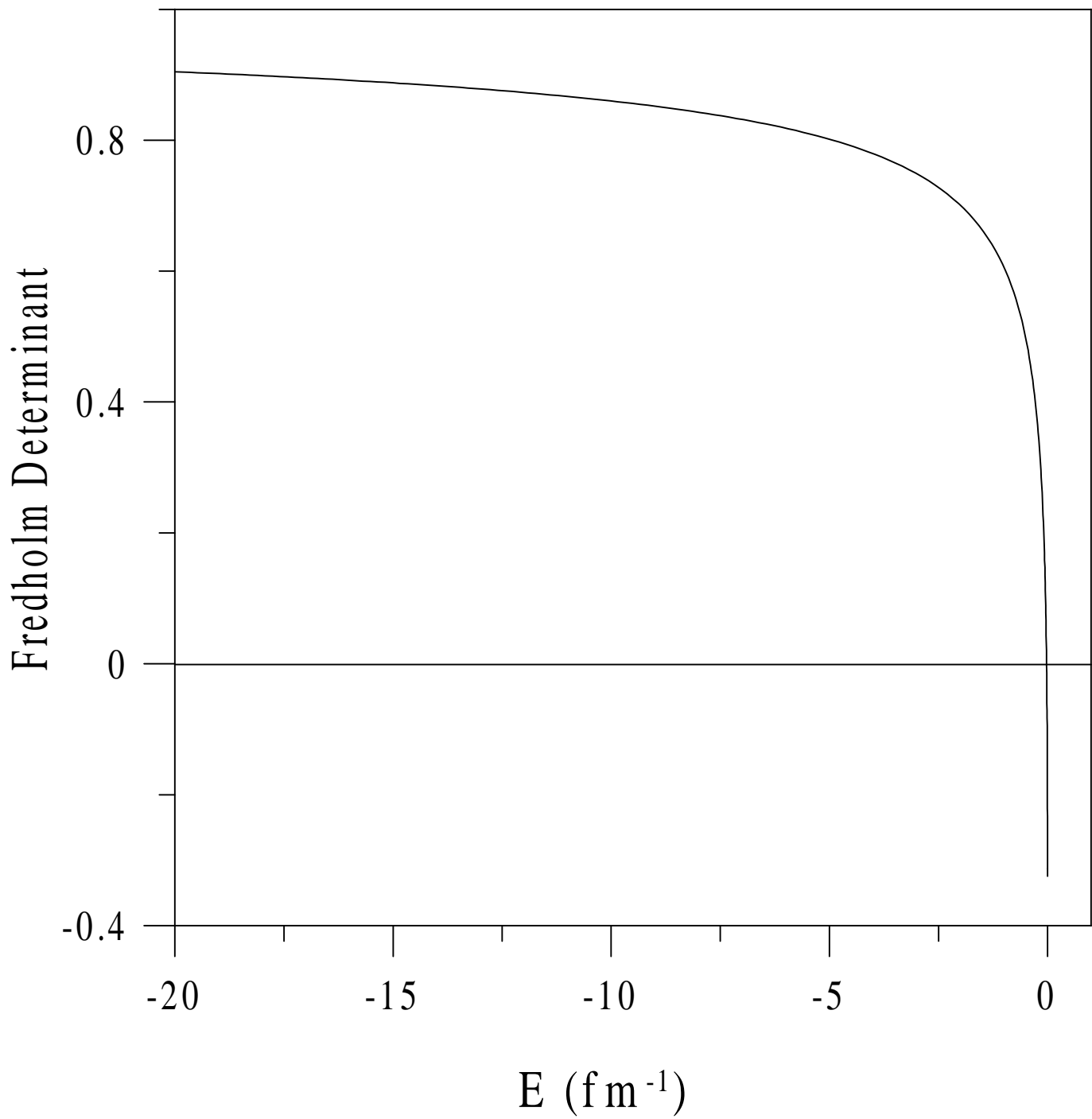


Figure 2

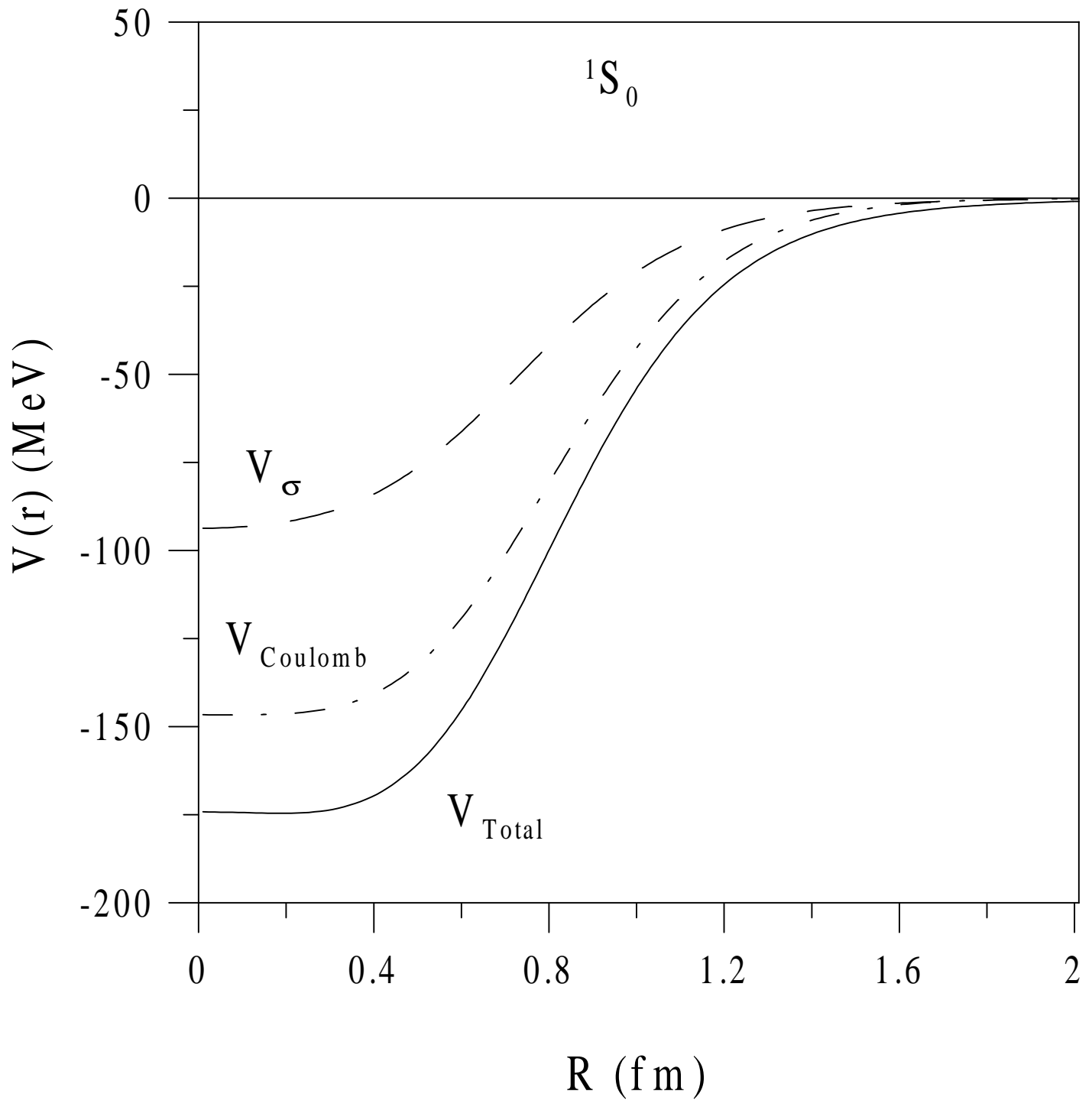


Figure 3

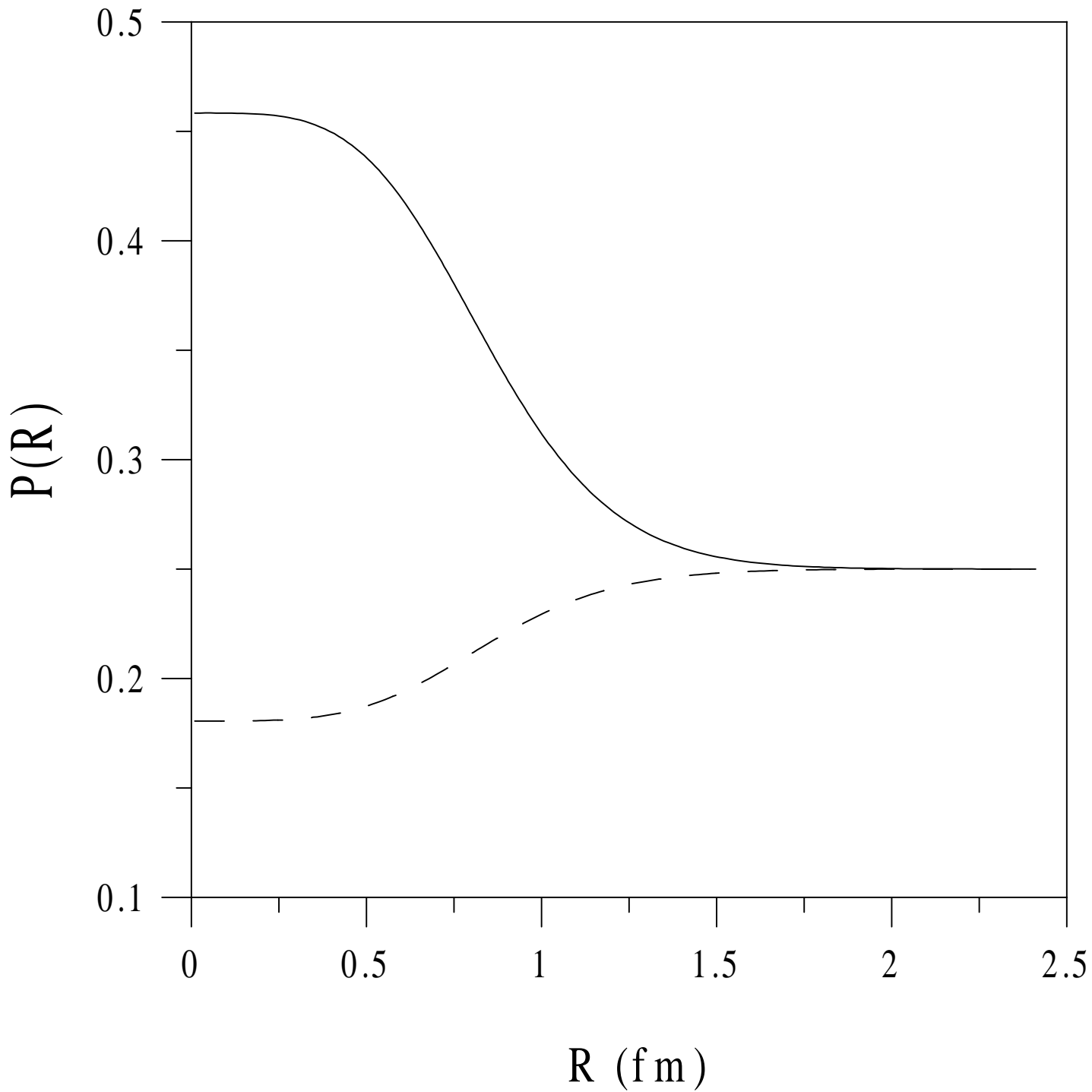


Figure 4

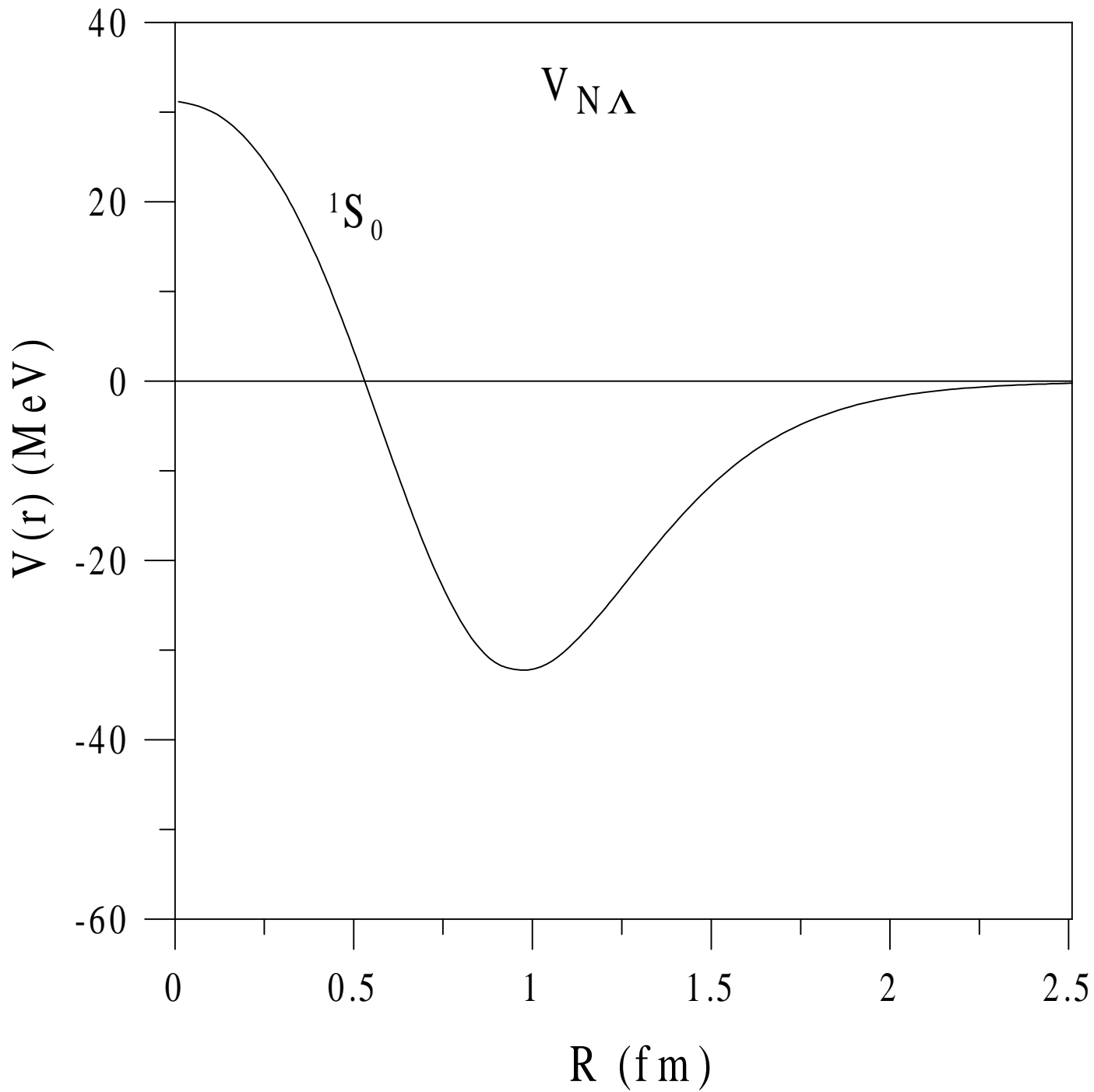


Figure 5

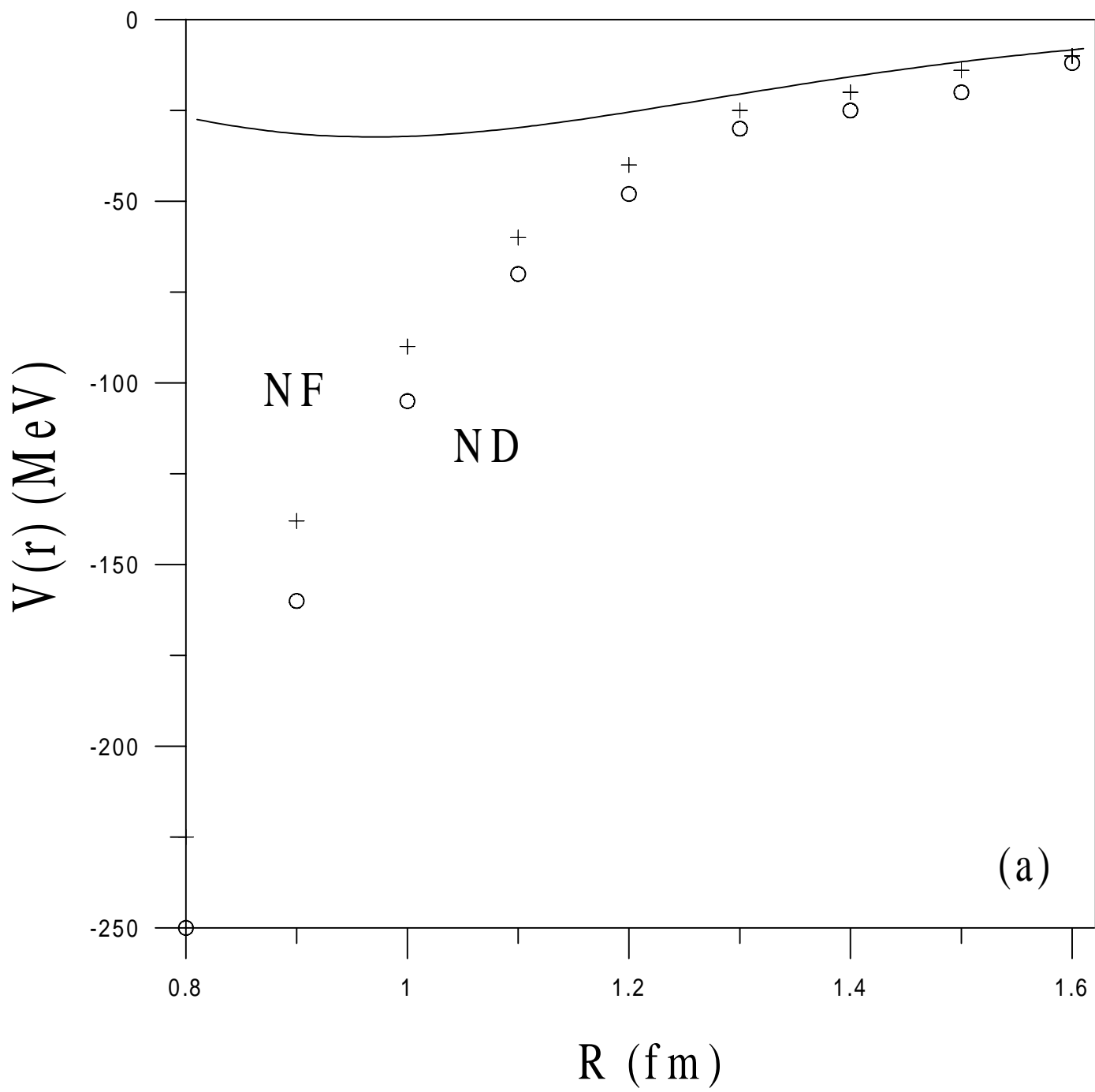


Figure 6

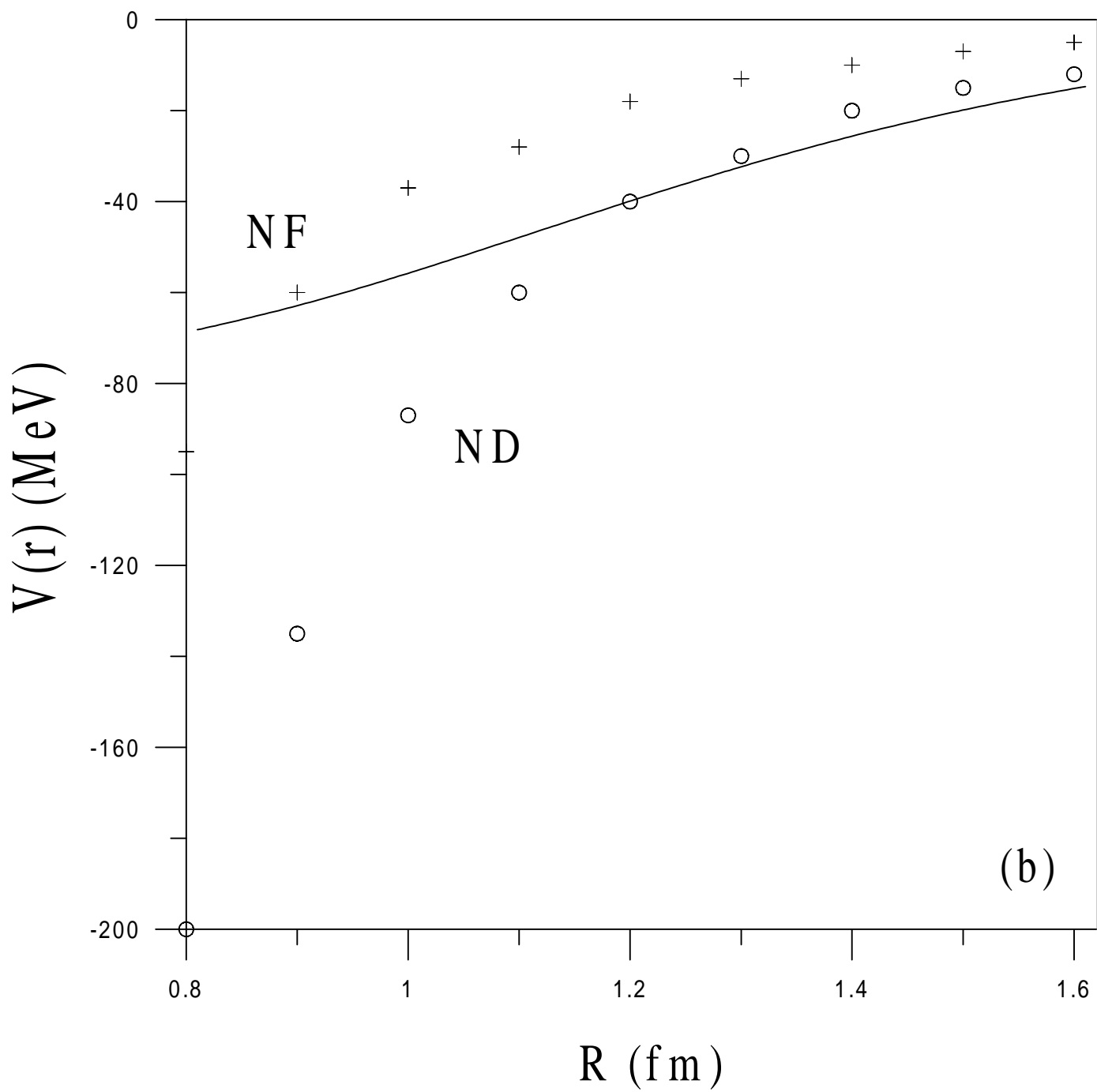


Figure 6